Multi-Frequency Search for Dark Matter in Cosmic Structures

Sergio Colafrancesco *

INAF - Osservatorio Astronomico di Roma
Via Frascati 33, I-00040 Monteporzio (Roma), Italy

Abstract We discuss here the constraints on the Dark Matter (DM) nature that can be obtained from a multi-frequency study of the annihilation of DM particles in cosmic structures on large scales. We discuss specifically the predictions of SUSY neutralino models.

Key words: Cosmology: Dark Matter — galaxies: galaxy clusters: dwarf galaxies

1 INTRODUCTION. THE DARK UNIVERSE

There is evidence (Spergel et al. 2003, Riess et al. 1998, Perlmutter et al. 1999) that we live in a flat ($\Omega_0 \approx 1$), dark universe dominated by Dark Matter (DM) and Dark Energy (DE). Dark Matter provides a fraction $\Omega_m \approx 0.23 \pm 0.04$ of the overall matter-energy content (the rest being provided by Dark Energy with $\Omega_{\rm DE} \approx 0.73 \pm 0.04$ with the baryonic contribution limited to $\Omega_{\rm b} \approx 0.044 \pm 0.004$) and amounts to $\sim 85\%$ of the total mass content of the universe. There are five basic properties that DM is observed to have: *i)* DM is not observed to shine (it is nearly dissipationless), implying that DM particles have very weak e.m. interactions; *ii)* DM is nearly collisionless, as indicated by the approximate triaxiality of DM halos (e.g., galaxy cluster); *iii)* DM is cold to reproduce the observed properties of galaxies and galaxy formation; *iv)* DM is considered as a fluid on galaxy scales such that a would-be discreteness is not detectable yet; *v)* DM behaves in a classical way to be confined on galaxy scales. The first three aspects do not place any constraint on the space of possibilities, while the last two place upper and lower limits, respectively, on the mass of the DM particles.

It is not surprising that most of the matter in the universe should be dark: there is no reason why everything in the universe should shine, and it has been not difficult to think of possible candidates (Baltz 2004). Obviously, direct detection is the cleanest and most decisive discriminant (see, e.g., Munoz 2004 for a review). However, it would be especially interesting if astronomical techniques were to reveal some of the fundamental particles properties predicted by theorists. If such particles turn out to account for the DM, we would have to view the galaxies, clusters of galaxies and large-scale structures in a downgraded perspective.

The dark side of the universe sends us signals of the presence and of the nature nature of DM that can be recorded using different astrophysical probes. These probes are of *inference* and *physical* character. Inference probes tell us about the presence, the total amount and the spatial distribution of DM in the large scale structures but cannot provide detailed information on the nature of DM. Physical probes tell us about the nature and the physical properties of the DM particles and can be obtained by studying the astrophysical signals of their interaction/annihilation in the atmospheres of DM-dominated structures (like galaxy cluster and galaxies). These probes can be recorded over a wide range of frequencies from radio to gamma-rays and prelude to a full multi-frequency search for the nature of DM in cosmic structures.

2 INFERENCE PROBES

Inference probes of DM are, e.g., the CMB anisotropy spectrum (e.g., Spergel et al. 2003), the dynamics of galaxies (e.g., Zwicky 1933), the hydrodynamics of the hot intra-cluster gas (e.g., Arnaud 2005 for a review) and the gravitational lensing distortion of background galaxies by the intervening potential wells of

* E-mail: `Sergio.Colafrancesco@mporzio.astro.it`

galaxy clusters (see Bartelmann & Schneider 1999 for a review). These probes tell us about the presence, the total amount and the spatial distribution of DM in the large scale structures, from galaxies to clusters of galaxies and to the overall universe.

The CMB can be considered as the largest detector for DM. In fact, the multipole structure of its anisotropy spectrum depends on the overall amount of DM in the universe and the acoustic peaks are sensitive to the energy density ratio of DM to radiation (e.g., Bennett et al. 2003, Spergel et al. 2003, Hu & Dodelson 2002).

Other estimates of the amount and distribution of DM in the universe come from the study of large scale structures at a more recent epoch in the cosmic evolution (see, e.g., Seljak et al. 2004). The reason why cosmic structures contain a record of the DM distribution in the universe is due to the fact that the evolution of the parent density perturbations has been dominated by their DM content. The study of galaxies and galaxy clusters - the largest gravitationally bound structures in the universe whose potential wells are dominated by DM - provides information on both the amount of DM and on its spatial distribution. Numerical simulations indicate that virialized DM halos on the scales of galaxies and galaxy clusters show a cuspy density profile, generally represented by a density profile

$$\rho(r) = \rho_0 g(r) \ \text{ with } \ g(r) = \left(\frac{r}{r_c}\right)^{-\eta}\left(1 + \frac{r}{r_c}\right)^{\eta-\xi}, \tag{1}$$

where $\eta = 1$ and $\xi = 3$ reproduce the NFW (Navarro, Frenk & White 1997,2004) DM density profile. Actually, the inner DM density profile found in N-body simulations can take slopes in a wider range, $r^{-0.5} - r^{-1.5}$, and it can be flattened or steepened by the presence of a baryonic feedback on DM (Gnedin & Primack 2004) or a DM–DE coupling (Macció et al. 2004). Observations of the inner parts of galaxies reveal that the DM density profile at scales $r \lesssim 1\,\text{kpc}$ from the galaxy center is much flatter than the NFW profile and that there is no evidence of a cusp at $r \lesssim 0.2\,\text{kpc}$. At $r \lesssim 2\,\text{pc}$, the supermassive Black-Hole supposed to be at the galaxy centers dominates the galactic dynamics, and its interaction with the surrounding medium may lead to a complex density profile (Gnedin & Primack 2004). Temperature profiles observed in E-galaxies with Chandra from ~ 0.7 to $\sim 35\,\text{kpc}$ (as in NGC 4636) indicate that the composite mass distribution has a steep slope with no core (Lowenstein et al. 2002). Based on the available evidence, we should state that there is not yet a definitive conclusion on the shape of the DM density profile in the central regions of galaxies. Observations of galaxy cluster do not help much in this respect since the available data stop our understanding of the DM density profile at distances $r \sim 10\,\text{kpc}$ from their centers (Buote 2003). Down to these scales the NFW is still allowed and at smaller scales the inner slope remains quite uncertain even when the combined analysis of X-ray, gravitational lensing and galaxy dynamics data are taken into account (Dalal & Keaton 2003). On the theoretical side, the uncertainty in the modeling of the DM distribution is enhanced by at least two issues: i) the cusp problem may be alleviated by changes in the basic physics (e.g., self-interaction of DM particles with large annihilation cross section, broken scale-invariance, modified gravity) or by the baryon-DM coupling and interaction (e.g., gas outflow during early stages of galaxy formation); ii) the cusp problem may be strengthened by the possible DM–DE coupling (e.g., modified particle dynamics).

To summarize, inference probes can be used to assess the presence, the amount and the spatial distribution of DM in large scale structures but are not able to provide specific information on its nature.

3 PHYSICAL PROBES

The nature of the DM basic constituents is still unknown. Among the viable competitors for having a cosmologically relevant DM species, the leading candidate is the lightest supersymmetric (SUSY) particle, plausibly the neutralino χ, with a mass M_χ in the range between a few GeV to a few hundreds of GeV (see Baltz 2004 for a recent review). Physical probes of the nature of the DM particles tell us about their nature and physical properties and can be obtained by studying the astrophysical signals of their interaction/annihilation in the halos of cosmic structures (galaxy clusters and/or galaxies). These signals involve, in the case of a χ DM, emission of gamma-rays, neutrinos, together with the synchrotron and bremsstrahlung

radiation and the Inverse Compton Scattering (ICS) of the CMB (and other background) photons by the secondary electrons produced in the DM annihilation process (see Fig. 1). [1]
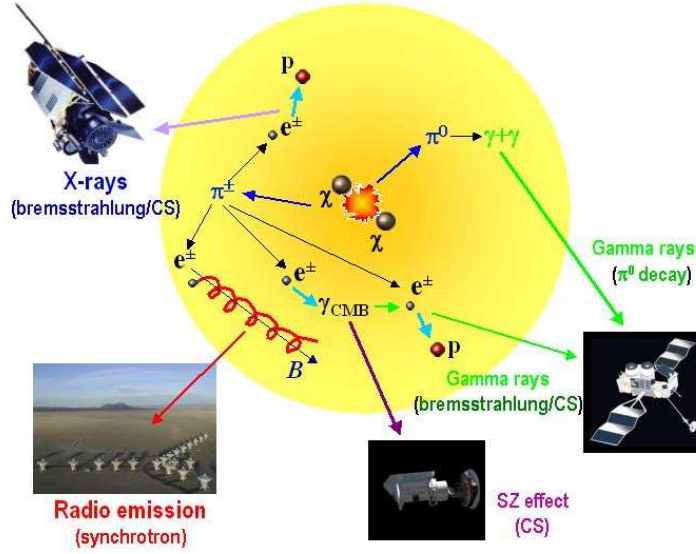
Fig. 1 A simple model which shows the basic astrophysical mechanisms underlying the search for the nature of DM particles (χ) through the emission features occurring in large-scale structures (e.g., galaxy clusters and galaxies). These mechanisms are, among others: γ-ray emission from $\pi^0 \to \gamma + \gamma$, relativistic bremsstrahlung of secondary $e^\pm$ and ICS of CMB photons by secondary $e^\pm$; X-ray/UV emission due to non-thermal bremsstrahlung and ICS of background photons by secondary $e^\pm$; synchrotron emission by secondary $e^\pm$ diffusing in the intra-cluster magnetic field; SZ_{DM} (ICS of CMB photons by secondary $e^\pm$) effect.

The χ annihilation rate is $R = n_\chi(r)\langle\sigma v\rangle$, where $n_\chi(r) = n_{\chi,0} g(r)$ is the neutralino number density and $\langle\sigma v\rangle$ is the $\chi\chi$ annihilation cross section averaged over a thermal velocity distribution at freeze-out temperature (Jungman et al. 1996). The range of neutralino masses and pair annihilation cross sections in the most general supersymmetric DM setup is extremely wide. Neutralinos as light as few GeV (see Bottino et al. 2003) and as heavy as hundreds of TeV (see Profumo 2005) can account for the observed CDM density through thermal production mechanisms, and essentially no constraints apply in the case of non-thermally produced neutralinos. Turning to the viable range of neutralino pair annihilation cross sections, coannihilation processes do not allow to set any lower bound, while on purely theoretical grounds a general upper limit on $\langle\sigma v\rangle \lesssim 10^{-22}(M_\chi/\text{TeV})^{-2} \text{ cm}^3 \text{ s}^{-1}$ has been recently set (Profumo 2005). The only general argument which ties the relic abundance of a WIMP with its pair annihilation cross section is given by the naive relation

$$\Omega_\chi h^2 \simeq (3 \times 10^{-27} \text{ cm}^3 \text{ s}^{-1})/\langle\sigma v\rangle, \tag{2}$$

(see Jungman et al. 1996), which points at a fiducial value for $\langle\sigma v\rangle \simeq 3 \times 10^{-26} \text{ cm}^3 \text{ s}^{-1}$. The above mentioned relation can be, however, badly violated in the general MSSM, or even within minimal setups, such as the minimal supergravity scenario (see discussion in Colafrancesco et al. 2005). We will consider here two reperesentative SUSY models for discussion: a soft $b\bar{b}$ model with $M_\chi = 40$ GeV and a hard W^+W^- model with $M_\chi = 81$ GeV, with their appropriate annihilation cross-sections (see Colafrancesco et al. 2005 for details). Enhancing (suppressing) the χ annihilation rate will have the simple effect of rescaling the final secondary products ($e^\pm, \pi^{0,\pm}$) spectra by the same enhancement (suppression) factor.

---

[1] DM annihilation produces several types of particle and anti-particle fluxes, whose complete description is not discussed here for the sake of brevity. We refer the interested reader to Colafrancesco, Profumo & Ullio 2005.

Neutralinos which annihilate inside a DM halo produce quarks, leptons, vector bosons and Higgs bosons, depending on their mass and physical composition. Electrons are then produced from the decay of the final heavy fermions and bosons. The different composition of the $\chi\chi$ annihilation final state will in general affect the form of the electron spectrum. Both detailed MonteCarlo calculations of the $e^\pm$ spectrum (CPU 2005) and analytical, approximated expressions (Colafrancesco & Mele 2001) have been given in the literature, and we refer to these papers for details.

Gamma-rays produced by neutral pion decay, $\pi^0 \to \gamma\gamma$, generate most of the continuum spectrum at energies $E \gtrsim 1\,\text{GeV}$ and this emission is directly radiated since the $\pi^0 \to \gamma\gamma$ e.m. decay is very fast. This gamma-ray emission is dominant at high energies, $\gtrsim 0.3 - 0.5$ of the neutralino mass, but needs to be complemented by other two emission mechanisms which produce gamma-rays at similar or slightly lower energies: these are the ICS and the bremsstrahlung emission by secondary electrons (see Sect. 3.1 below).

Secondary electrons are produced through various prompt generation mechanisms and by the decay of charged pions (see, *e.g.*, Colafrancesco & Mele 2001). In fact, charged pions decay through $\pi^\pm \to \mu^\pm \nu_\mu(\bar\nu_\mu)$, with $\mu^\pm \to e^\pm + \bar\nu_\mu(\nu_\mu) + \nu_e(\bar\nu_e)$ and produce $e^\pm$, muons and neutrinos. Electrons and positrons are produced abundantly by neutralino annihilation and are subject to spatial diffusion and energy losses. Both spatial diffusion and energy losses contribute to determine the evolution of the source spectrum into the equilibrium spectrum of these particles, *i.e.* the quantity which will be used to determine the overall multi-wavelength emission induced by DM annihilation. The secondary electrons eventually produce radiation by synchrotron in the magnetized atmosphere of Coma, Inverse Compton Scattering of CMB (and other background) photons and bremsstrahlung with protons and ions in the atmosphere of the Coma cluster (see, *e.g.*, Colafrancesco 2004a, 2005a for reviews). These secondary particles also produce heating of the intra-cluster gas by Coulomb collisions with the intra-cluster gas particles and SZ effect (see, *e.g.* Colafrancesco 2004b, 2005a).

The time evolution of the secondary electron spectrum is described by the transport equation:

$$\frac{\partial n_e}{\partial t} = \nabla\left[D\nabla n_e\right] + \frac{\partial}{\partial E}\left[b_e(E)n_e\right] + Q_e(E,r) , \qquad (3)$$

where $n_e(E,r)$ is the equilibrium spectrum at distance r from the cluster center for the electrons with energy E. To get a more physical insight on the relevance of spatial diffusion in large-scale structures, it is useful to consider the following qualitative solution for the average electron density

$$\frac{dn_e(E,r)}{dE} \approx \left[Q_e(E,r)\tau_{\text{loss}}\right] \times \frac{V_s}{V_s + V_o} \times \frac{\tau_D}{\tau_D + \tau_{\text{loss}}} , \qquad (4)$$

(see, *e.g.*, Colafrancesco 2005b) which resumes the relevant aspects of the transport equation (Eq. 3). Here, $V_s \propto R_h^3$ and $V_o \propto \lambda^3(E)$ are the volumes occupied by the DM source and the one occupied by the diffusing electrons which travel a distance $\lambda(E) \approx [D(E) \cdot \tau_{\text{loss}}(E)]^{1/2}$ before loosing much of their initial energy. The relevant time scales in Eq. (3) are the diffusion time-scale, $\tau_D \approx R_h^2/D(E)$, and the energy loss time-scale $\tau_{\text{loss}} = E/b_e(E)$, where D is again the diffusion coefficient for which we can assume the generic scaling $D(E) = \tilde{D}_0(E/E_0)^\gamma B^{-\gamma}$, and $b(E)$ the electron energy loss per unit time at energy E.

For $E > E_* = (\tilde{D}_0 E_0/R_h^2 b_0 B_\mu^\gamma)^{1/(1-\gamma)}$ (for simplicity we have kept leading terms only, implementing $b(E) \simeq b_0(B_\mu)(E/\text{GeV})^2 + b_{\text{Coul}})$, the condition $\tau_D > \tau_{\text{loss}}$ (and consistently $\lambda(E) < R_h$) holds, the diffusion is not relevant and the solution of Eq. (3) is $dn_e/dE \sim Q_e(E,r)\tau_{\text{loss}}$ and shows an energy spectrum $\sim Q(E) \cdot E^{-1}$. This situation ($\lambda(E) < R_h, \tau_D > \tau_{\text{loss}}$) applies to the regime of galaxy clusters.

For $E < E_*$, the condition $\tau_D < \tau_{\text{loss}}$ (and consistently $\lambda(E) > R_h$) holds, the diffusion is relevant and the solution of Eq. (3) is $dn_e/dE \sim [Q_e(E,r)\tau_D] \times (V_s/V_o)$ and shows an energy spectrum $\sim Q(E) \cdot E^{(2-5\gamma)/2}$ which is flatter or equal to the previous case for reasonable values $\gamma = 1/3 - 1$. This last situation ($\lambda(E) > R_h, \tau_D < \tau_{\text{loss}}$) applies to the regime of dwarf galaxies (see Colafrancesco 2005b, Colafrancesco et al. 2005). In conclusion, diffusion can be neglected in galaxy clusters while it is relevant on galactic and sub-galactic scales (Colafrancesco et al. 2005).

The DM source spectrum, $Q_e(E,r)$, is constant over time and the population of high-energy $e^\pm$ in galaxy clusters can be described by a quasi-stationary ($\partial n_e/\partial t \approx 0$) transport equation from which $n_e(E,r)$ reaches its equilibrium configuration mainly due to synchrotron and ICS losses at energies $E \gtrsim 150\,\text{MeV}$

and to Coulomb losses at smaller energies (Colafrancesco & Mele 2001, Colafrancesco et al. 2005). The $e^\pm$ energy loss per unit time, b_e (in units of GeV s^{-1}), at energy E is $b_e = b_{ICS} + b_{synch} + b_{brem} + b_{Coul}$, where $b_{ICS} \approx 2.5 \times 10^{-17}(E/\text{GeV})^2$, $b_{synch} \approx 2.54 \times 10^{-18}B_\mu^2 \, (E/\text{GeV})^2$, $b_{brem} \approx 1.51 \times 10^{-16}$ $(n/\text{cm}^{-3})\,(\log(\Gamma/n) + 0.36)$, $b_{Coul} \approx 7 \times 10^{-16}(n/\text{cm}^{-3})\,(1 + \log(\Gamma/n)/75)$, n is the intracluster gas density and $\Gamma \equiv E/m_e c^2$.

3.1 The multi-ν Spectral Energy Distribution from DM annihilation

The astrophysical signals of DM annihilation can be visible over the entire e.m. spectrum, from radio to γ-ray frequencies (see Fig. 2).
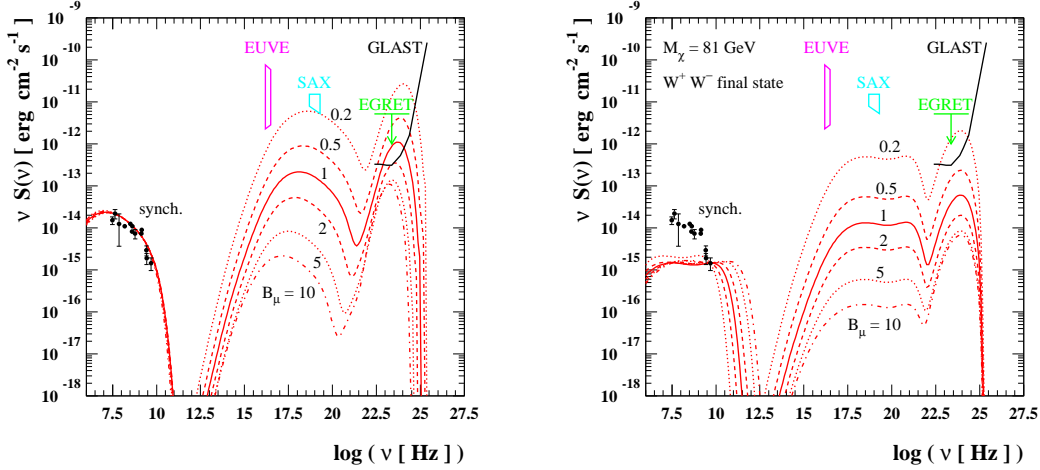
Fig. 2 Multi-frequency spectrum of the two best fit models of the radio halo flux of Coma: $M_\chi = 40\,\text{GeV}$ ($b\bar{b}$; left) and $M_\chi = 81\,\text{GeV}$ (W^+W^-; right). The halo profile is the best fit Navarro (2004 1997,2004) profile with $M_{vir} = 0.9 \times 10^{15} M_\odot h^{-1}$ and $c_{vir} = 10$, with subhalo setup as given by Colafrancesco et al.(2005). The scaling of the multi-frequency spectrum with the value for the mean magnetic field B_μ in Coma is shown for the two representative neutralino DM models.

Gamma rays. Gamma-ray emission is predominantly due to the hadronization of the decay products of $\chi\chi$ annihilation with a continuum γ-ray spectrum due to the decay $\pi^0 \to \gamma + \gamma$ (Colafrancesco & Mele 2001, Colafrancesco et al. 2005), even though the direct neutralino annihilation results in a line emission feature at an energy $\sim M_\chi$. Gamma-ray emission is also expected from secondary $e^\pm$ produced by $\chi\chi$ annihilation via $\chi\chi \to \pi^\pm + X$, $\pi^\pm \to \mu^\pm \nu_\mu(\bar{\nu}_\mu)$, $\mu^\pm \to e^\pm + \bar{\nu}_\mu(\nu_\mu) + \nu_e(\bar{\nu}_e)$. These secondary $e^\pm$ may produce γ-rays through bremsstrahlung and ICS of CMB photons up to high energies (see Fig. 2). Gamma-ray emission is the most direct signal of DM annihilation. It could be revealed provided that i) sufficient spectral and spatial resolution will be achieved by the upcoming experiments and ii) a clear understanding of other competing emission mechanisms (like cosmic-ray acceleration) expected to work in DM halos (Colafrancesco 2005a for a review) will be obtained.

The gamma-ray flux produced by this model is dominated by the continuum $\pi^0 \to \gamma\gamma$ component and it is a factor ~ 5 lower than the EGRET upper limit of Coma at its peak frequency (see Fig. 2, left panel). Such gamma-ray flux could be, nonetheless, detectable by the GLAST–LAT detector at its peak energy (we will discuss more specifically the detectability of the gamma-ray WIMP annihilation signals from galaxy clusters in a dedicated, forthcoming paper (Colafrancesco et al. 2005). The rather low neutralino mass $M_\chi = 40\,\text{GeV}$ of this model makes it rather difficult to be testable by Cherenkov gamma-ray detectors operating at higher threshold energies.

Radio emission. The secondary $e^\pm$ produced by $\chi\chi$ annihilation can produce synchrotron emission in the magnetized atmosphere of galaxy clusters (as well as galaxies) which coild be observed at radio frequencies as a diffuse radio emission centered on the DM halo. Observations of cluster radio-halos are, in principle, very effective in constraining the neutralino mass and composition (Colafrancesco & Mele 2001, Colafrancesco et al. 2005), under the hypothesis that DM annihilation provides a major contribution to the radio-halo flux (see a general discussion in Colafrancesco 2005a). Under this hypothesis, a pure energy requirement says that the neutralino mass is bound to be $M_\chi \geq 23.4\,\mathrm{GeV}(\nu/\mathrm{GHz})^{1/2}(B/\mu\mathrm{G})^{-1/2}$ in order that the secondary $e^\pm$ emit at frequencies $\nu \geq 1\,\mathrm{GHz}$, as observed in cluster radio halos (see Fig. 2). The available data indicate that a neutralino responsible for the cluster radio-halo emission should have $M_\chi \gtrsim 40\,\mathrm{GeV}$ and should annihilate predominantly into fermions (e.g., Colafrancesco & Mele 2001, Colafrancesco et al. 2005), consistently with the available accelerator limits. The best fit model ($b\bar{b}$ with $M_\chi = 40\,\mathrm{GeV}$) is able to reproduce both the overall radio-halo spectrum of Coma and the spatial distribution of its surface brightness (see Fig. 3).
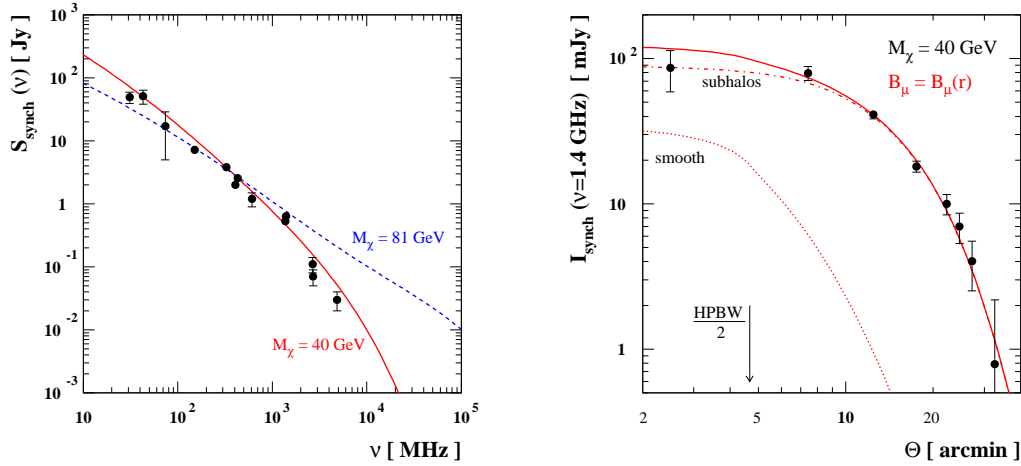
Fig. 3 Left. Best fit models for the radio flux density spectrum, in case of a soft spectrum due to a $b\bar{b}$ annihilation final state (solid line, model with $M_\chi = 40$ GeV) and of a hard spectrum due to a W^+W^- channel (dashed line, model with $M_\chi = 81$ GeV); values of all parameters setting the model are given in the text. Right. Surface brightness distribution at $\nu = 1.4$ GHz, within a beam equal to $9'.35$ (HPBW), for the the lightest WIMP model. We consider an observationally driven model with magnetic field $B(r) = B_0\left(1 + \frac{r}{r_{c1}}\right)^2 \cdot \left[1 + \left(\frac{r}{r_{c2}}\right)^2\right]^{-\beta}$ with $B_0 = 0.55\,\mu$G, $\beta = 2.7$, $r_{c1} = 3'$ $r_{c2} = 17'.5$ in order to reproduce the measured surface brightness. In both cases, the contributions from the smooth dark matter halo component only and from substructures only are also displayed (see Colafrancesco et al. 2005 for details).

An appealing property of the WIMP model worked out here is that it can reproduce both the spectral and the spatial distribution of the radio-halo features of Coma. As for the radio-halo surface brightness profile, it seems necessary for this WIMP model - due to the shape of the DM halo profile - to invoke a radial distribution of the magnetic field with a mild decrease towards the Coma center to counterbalance the centrally peaked DM profile, and with an exponential cutoff at large radii to counterbalance the effect of the subhalo distribution. We notice here that such a specific $B(r)$ spatial distribution is - interestingly enough - able to reproduce the radial distribution of the RMs in Coma (see Colafrancesco et al. 2005).

ICS of CMB: from infrared to gamma-rays For the best-fit values of $M_\chi = 40\,\mathrm{GeV}$ and $\langle\sigma v\rangle = 4.7 \times 10^{-25}\,\mathrm{cm}^3\,\mathrm{s}^{-1}$, with $B_\mu = 1.2$ this neutralino model yields EUV and HXR fluxes which are more than one order of magnitude fainter than the Coma data (see Fig. 2). Increasing the neutralino mass does not

provide a decent fit of the radio-halo spectrum (see Fig. 2, right panel) and yields, in addition, extremely faint EUV, HXR and gamma-ray fluxes, which turn out to be undetectable even by GLAST and/or by the next coming high-energy experiments. It is possible to recover the EUV and HXR data on Coma with a IC flux by secondary electrons by increasing the annihilation cross-sections by a factor $\sim 10^2$ (i.e., up to values $\langle \sigma v \rangle \approx 7 \times 10^{-23}$ cm^3 s^{-1}) in the best-fit $b\bar{b}$ soft WIMP model (at fixed $M_\chi = 40$ GeV). However, in such a case both the radio-halo flux and the hard gamma-ray flux at ~ 1 GeV as produced by π^0 decay should increase by the same factor leading to a problematic picture: in fact, while the radio-halo data would imply lower values of the magnetic field $B \sim 0.1$ μG which might still be allowed by the data, the $\pi^0 \rightarrow \gamma\gamma$ gamma-ray flux at $E > 100$ MeV should exceed the EGRET limit on Coma. This option is therefore excluded by the available data.

Alternatively, it would be possible to fit the EUV and HXR spectra of Coma with the adopted value of $\langle \sigma v \rangle \approx 7 \times 10^{-23}$ cm^3 s^{-1} for the $b\bar{b}$ model with $M_\chi = 40$ GeV, in the case we sensibly lower the mean magnetic field. Values of the average magnetic field $\lesssim 0.2\mu$G are required to fit the HXR flux of Coma under the constraint to fit at the same time the radio-halo spectrum (see Fig. 2, left panel), consistently with the general description of the ratio between the synchrotron and IC emission powers in Coma (see, *e.g.*, Colafrancesco et al.2005 for a discussion). Magnetic fields as low as $\sim 0.15\mu$G can fit both the HXR and the EUV fluxes of Coma. However, also in this case the $\pi^0 \rightarrow \gamma\gamma$ gamma-ray flux predicted by the same model at $E > 100$ MeV exceeds the EGRET limit on Coma, rendering untenable also this alternative. Actually, the EGRET upper limit on Coma set a strong constraint on the combination of values B and $\langle \sigma v \rangle$ (see Fig. 2, right panel) so that magnetic field larger than $\gtrsim 0.3$ μGare required for the parameter setup of the $b\bar{b}$ model with $M_\chi = 40$ GeV. Figure 2 shows the upper limits on the value of $\langle \sigma v \rangle$ as a function of the assumed value of the mean magnetic field of Coma.

According to these results, it is impossible to fit all the available data on Coma for a consistent choice of the DM model and of the cluster magnetic field. The EUV and HXR data in particular require extreme conditions, i.e. low values of the magnetic field and/or high values of the annihilation cross section, which violate the EGRET gamma-ray limit. Thus, realistic DM models that are consistent with the radio and gamma-ray constraints predict IC emission which falls short of fitting the EUV and HXR data of Coma.

A new probe: SZ effect from DM annihilation. The energetic electrons and positrons produced by WIMP annihilation interact with the CMB photons and up-scatter them to higher frequencies producing a peculiar SZ effect (as originally realized by Colafrancesco 2004b) with specific spectral and spatial features. The generalized expression for the SZ effect which is valid in the Thomson limit for a generic electron population (in the relativistic limit) and includes also the effects of multiple scatterings and the combination with other electron population in the cluster atmospheres has been derived by Colafrancesco et al. 2003. According to these results, the DM induced spectral distortion can be written as

$$\Delta I_{\mathrm{DM}}(x) = 2 \frac{(k_{\mathrm{B}} T_0)^3}{(hc)^2} y_{\mathrm{DM}} \, \tilde{g}(x) \, , \tag{5}$$

where T_0 is the CMB temperature and the Comptonization parameter y_{DM} is given by

$$y_{\mathrm{DM}} = \frac{\sigma_T}{m_e c^2} \int P_{\mathrm{DM}} d\ell \, , \tag{6}$$

in terms of the pressure P_{DM} contributed by the secondary electrons produced by neutralino annihilation. The quantity $y_{\mathrm{DM}} \propto \langle \sigma v \rangle n_\chi^2$ and scales as $\propto \langle \sigma v \rangle M_\chi^{-2}$, providing an increasing pressure P_{DM} and optical depth $\tau_{\mathrm{DM}} = \sigma_T \int d\ell n_e$ for decreasing values of the neutralino mass M_χ. The function $\tilde{g}(x)$, with $x \equiv h\nu/k_{\mathrm{B}} T_0$, for the DM produced secondary electron population can be written as

$$\tilde{g}(x) = \frac{m_e c^2}{\langle k_{\mathrm{B}} T_e \rangle} \left\{ \frac{1}{\tau} \left[\int_{-\infty}^{+\infty} i_0(x e^{-s}) P(s) ds - i_0(x) \right] \right\} \, , \tag{7}$$

in terms of the photon redistribution function $P(s)$ and of $i_0(x) = 2(k_{\mathrm{B}} T_0)^3/(hc)^2 \cdot x^3/(e^x - 1)$, where we defined the quantity

$$\langle k_{\mathrm{B}} T_e \rangle \equiv \frac{\sigma_{\mathrm{T}}}{\tau} \int P d\ell = \frac{\int P d\ell}{\int n_e d\ell} = \int_0^\infty dp f_e(p) \frac{1}{3} p v(p) m_e c, \tag{8}$$
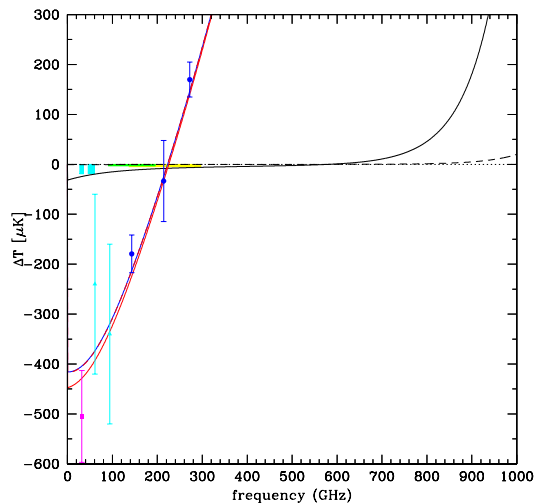
Fig. 4 The SZ effect produced by the $b\bar{b}$ model with $M_\chi = 40$ GeV (black solid curve) and by the W^+W^- model with $M_\chi = 81$ GeV (black dashed curve) in Coma are shown in comparison with the thermal SZ effect of Coma (blue curve). The red curves represent the overall SZ effect. Notice that the DM-induced SZ effect has a very different spectral behavior with respect to the thermal SZ effect. SZ data are from OVRO (magenta), WMAP (cyan) and MITO (blue). The sensitivity of PLANCK (18 months, 1 σ) is shown for the LFI detector at 31.5 and 53 GHz channels (cyan shaded regions) and for the HFI detector 143 and 217 GHZ channels (green and yellow shaded areas, respectively).

(see Colafrancesco 2004b) which is the analogous of the average temperature for a thermal population (for a thermal electron distribution $\langle k_B T_e \rangle = k_B T_e$ obtains, in fact). The photon redistribution function $P(s) = \int dp f_e(p) P_s(s; p)$ with $s = \ln(\nu'/\nu)$, in terms of the CMB photon frequency increase factor $\nu'/\nu = \frac{4}{3}\gamma^2 - \frac{1}{3}$, depends on the electron momentum (p) distribution, $f_e(p)$, produced by WIMP annihilation. We show in Figure 4 the frequency dependence of the temperature change,

$$\frac{\Delta T}{T_0} = \frac{(e^x - 1)^2}{x^4 e^x} \frac{\Delta I}{I_0} , \tag{9}$$

as produced by the DM-induced SZ effect in the two best fit WIMP models here considered, compared to the temperature change due to the thermal SZ effect produced by the intracluster gas. The most recent analysis of the thermal SZ effect in Coma (DePetris et al. 2003) provides an estimate of the optical depth of the thermal intracluster gas $\tau_{th} = 4.9 \times 10^{-3}$ which best fits the data. The model with $M_\chi = 40$ GeV provides a detectable SZ$_{DM}$ effect which has a very different spectral shape with respect to the thermal SZ effect: it yields a temperature decrement at all the microwave frequencies, $\lesssim 600$ GHz, where the thermal SZ effect is observed and produces a temperature increase only at very high frequencies > 600 GHz. This behavior is produced by the large frequency shift of CMB photons induced by the relativistic secondary electrons generated by the WIMP annihilation. As a consequence, the zero of the SZ$_{DM}$ effect is effectively removed from the microwave range and shifted to a quite high frequency ~ 600 GHz with respect to the zero of the thermal SZ effect, a result which allows, in principle, to estimate directly the pressure of the two electron populations and hence to derive constraints on the WIMP model (see Colafrancesco 2004b).

The presence of a substantial SZ$_{DM}$ effect is likely to dominate the overall SZ signal at frequencies $\nu \sim 220 - 250$ GHz providing a negative total SZ effect. It is, however, necessary to stress that in such frequency range there are other possible contributions to the SZ effect, like the kinematic effect and the non-thermal effect which could provide additional biases (see, *e.g.*, Colafrancesco et al. 2003). Nonetheless, the peculiar spectral shape of the SZ_{DM} effect is quite different from that of the kinematic SZ effect and of the thermal SZ effect and this result allows to disentangle it from the overall SZ signal. An appropriate multi-frequency analysis of the overall SZ effect based on observations performed on a wide spectral range

(from the radio to the sub-mm region) is required to separate the various SZ contributions and to provide an estimate of the DM induced SZ effect. In fact, simultaneous SZ observations at low frequencies $\sim 30\,\mathrm{GHz}$ (where there is the largest temperature decrement due to $\mathrm{SZ_{DM}}$), at $\sim 150\,\mathrm{GHz}$ (where the $\mathrm{SZ_{DM}}$ deepens the minimum in $\Delta I/I$ with respect to the dominant thermal SZ effect), at $\sim 220\,\mathrm{GHz}$ (where the $\mathrm{SZ_{DM}}$ dominates the overall SZ effect and produces a negative signal instead of the expected $\approx$ null signal) and at $\gtrsim 250\,\mathrm{GHz}$ (where the still negative $\mathrm{SZ_{DM}}$ decreases the overall SZ effect with respect to the dominant thermal SZ effect) coupled with X-ray observations which determine the gas distribution within the cluster (and hence the associated dominant thermal SZ effect) can separate the $\mathrm{SZ_{DM}}$ from the overall SZ signal, and consequently, set constraints on the WIMP model.

The WIMP model with $M_\chi = 40\,\mathrm{GeV}$ produces a temperature decrement which is of the order of ~ 40 to $15\,\mu\mathrm{K}$ for SZ observations in the frequency range ~ 30 to $150\,\mathrm{GHz}$ (see Fig. 4). These signals are still within the actual uncertainties of the available SZ data for Coma but, nonetheless, they could be detectable with higher sensitivity experiments. The high sensitivity planned for the future SZ experiments can provide much stringent limits to the additional SZ effect induced by DM annihilation. In this context, the next coming sensitive bolometer arrays (e.g., APEX) and the PLANCK-HFI experiment, or the planned OLIMPO balloon-borne experiment, have enough sensitivity to probe in details the contributions of various SZ effects in the frequency range $\nu \approx 30 - 250\,\mathrm{GHz}$, provided that accurate cross-calibration at different frequencies can be obtained. The illustrative comparison between the model predictions and the sensitivity of the PLANCK LFI and HFI detectors at the optimal observing frequencies ($\nu = 31.5$ and $53\,\mathrm{GHz}$ for the LFI detector and $\nu = 143$ and $217\,\mathrm{GHz}$ for the HFI detector) show that the study of the SZ effect produced by DM annihilation is actually feasible with the next generation SZ experiments. However, while the model with $M_\chi = 40\,\mathrm{GeV}$ provides a detectable signal which is a sensitive fraction of the thermal SZ effect at $\nu < 250\,\mathrm{GHz}$, the SZ signal provided by the model with $M_\chi = 81\,\mathrm{GeV}$ is by far too small to be detectable at any frequency.

The spectral properties shown by the $\mathrm{SZ_{DM}}$ for neutralinos depends on the specific neutralino model as we have shown in Figure 4: in fact, the SZ effect is visible for a neutralino with $M_\chi = 40\,\mathrm{GeV}$ and not visible for a neutralino with $M_\chi = 81\,\mathrm{GeV}$. Thus the detailed features of the SZ effect from DM annihilation depends strongly on the mass and composition of the DM particle, and - in turn - on the equilibrium spectrum of the secondary electrons. Each specific DM model predicts its own spectrum of secondary electrons and this influences the relative SZ effect. Models of DM which provide similar electron spectra will provide similar SZ effects.

Heating. Low energy secondary electrons produced by WIMP annihilation might heat the intracluster gas by Coulomb collisions since the Coulomb loss term dominates the energy losses at $E \lesssim 200\,\mathrm{MeV}$. The specific heating rate is given by

$$\frac{dE}{dt\,dV} = \int dE \frac{dn_\mathrm{e}}{dE} \cdot \left(\frac{dE}{dt}\right)_\mathrm{Coul}, \qquad (10)$$

where $\frac{dn_\mathrm{e}}{dE}$ is the equilibrium electron spectrum and the Coulomb loss rate is $(dE/dt)_\mathrm{Coul} = b^0_\mathrm{Coul} n \left(1 + \log(\gamma/n)/75\right)$ where n is the mean number density of thermal electrons in cm^{-3}, the average over space gives about $n \simeq 1.3 \times 10^{-3}$), $\gamma \equiv E/m_\mathrm{e}$ and we find $b^0_\mathrm{Coul} \simeq 6.13 \times 10^{-16}\,\mathrm{GeV\,s}^{-1}$.

Figure 5 shows the specific heating rate of Coma as produced in the two WIMP models which fit the radio data. The non-singular N04 halo model adopted in our analysis does not provide a high specific heating rate at the cluster center, and thus one might expect an overall heating rate for Coma which is of order of $\sim 10^{38}\,\mathrm{erg\,s}^{-1}$ ($\sim 10^{36}\,\mathrm{erg\,s}^{-1}$ for the WIMP model with $M_\chi = 40\,\mathrm{GeV}$ ($M_\chi = 81\,\mathrm{GeV}$). We also notice that the region that mostly contribute to the overall heating of Coma is not located at the center of the cluster. This is again a consequence of the non-singular N04 DM profile which has been adopted. The diffusion of electrons in the innermost regions of Coma acts in the same direction and moves the maximum of the curves shown in the right panel of Figure 5 towards the outskirts of Coma, even in the case of a halo density profile which is steeper than the adopted one.

This implies, in conclusions, that WIMP annihilation cannot provide most of the heating of Coma, even in its innermost regions. Such conclusion seems quite general and implies that non-singular DM halo
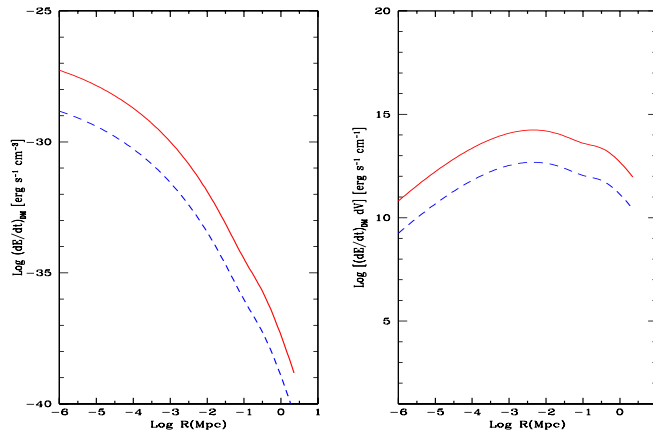
Fig. 5 Left: the specific heating rate is plotted against the radial distance from the center of Coma. Right: the specific heating rate multiplied by the volume element is plotted against the radial distance from the center of Coma.

models are not able to provide large quantities of heating at the centers of galaxy cluster so to quench efficiently the cooling of the intracluster gas (with powers of $\sim 10^{43} - 10^{45}$ erg s^{-1}). Only very steep halo profiles (even steeper than the Moore profile) and with the possible adiabatic growth of a central matter concentration (e.g., a central BH) could provide sufficient power to quench locally (*i.e.* in the innermost regions) the intracluster gas cooling (see, *e.g.*, Totani 2005). However, we stress that the spatial diffusion of the secondary electrons in the innermost regions of galaxy clusters should flatten the specific heating rate in the vicinity of the DM spike and thus decrease substantially the heating efficiency by Coulomb collisions. In conclusion, we believe that the possibility to solve the cooling flow problem of galaxy clusters by WIMP annihilation is still an open problem.

4 CONCLUSIONS

Viable WIMP models which are consistent with WMAP and with the structure of galaxy clusters are able to fit the Coma radio-halo data but produce relatively low intensity emission at EUV, X-ray and γ-ray frequencies. Gamma-rays from DM annihilation in Coma could be detectable by GLAST if $B \lesssim 2$ μG. These models also produce modest heating rates for the assumed non-singular DM halo profiles. The best-fit ($b\bar{b}$) WIMP model with $M_\chi = 40$ GeV predicts, nonetheless, a detectable SZ$_{\rm DM}$ effect at the level of $\sim$ 40 to 10 μK in the $\sim 30 - 150$ GHz range, which could be observable with the upcoming high-sensitivity microwave experiments. The constraints set by the SZ$_{\rm DM}$ effect on the $\langle \sigma v \rangle$-M_χ plane combined with the WMAP constraints on $\langle \sigma v \rangle$ further restrict the available neutralino models. Additional restrictions of this plane may be obtained by comparing the previous astrophysical constraints to the constraints coming from both accelerator physics and from other cosmological probes which are sensitive to the amount and nature of the DM. Along this line, we show in Figure 6 a scatter plots of the viable SUSY configurations, indicating with filled green circles those *thermally* producing a neutralino relic abundance within the 2-σ WMAP range, and with red circles those producing a relic abundance *below* the WMAP range (whose relic abundance can however be cosmologically enhanced, in the context of quintessential or Brans-Dicke cosmologies, or which can be non-thermally produced, as to make up all of the observed CDM. The regions of the $\langle \sigma v \rangle - M_\chi$ plan allowed by the data values are therefore shown to be actually populated by a number of viable SUSY models. Direct DM detection experiments have already explored large regions of the most optimistic SUSY models, and the planned next-generation experiments will probably be able to explore also the core of the SUSY models. In this context, we have shown that the astrophysical study of DM annihilation proves to be complementary, but hardly competitive, especially when a full multi-frequency approach is chosen. When combined with future accelerator results, such multi-frequency astrophysical search might greatly help us to unveil the elusive nature of Dark Matter.
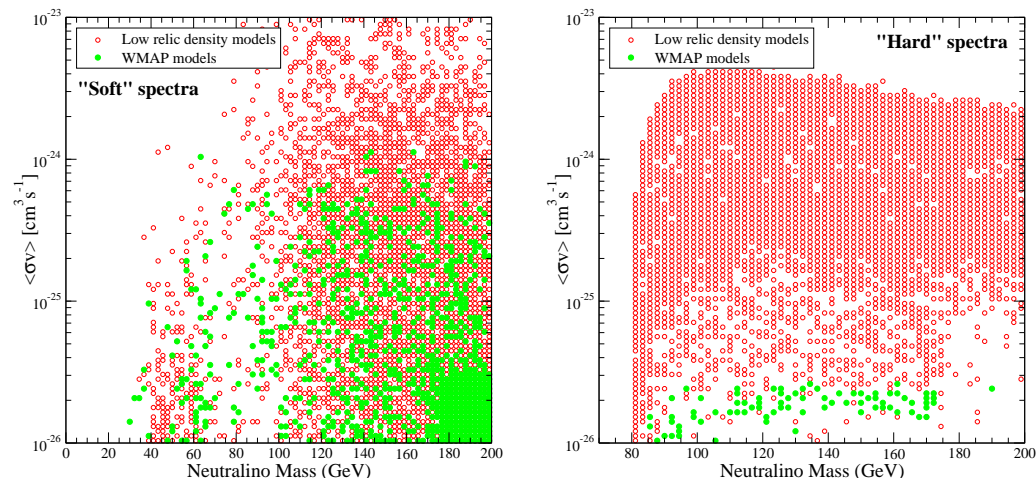
Fig. 6 A scatter plot of SUSY models, consistent with all available phenomenological constraints, giving a relic abundance in the 2-σ WMAP range (green filled circles) or below it (low, relic density models, red circles), for soft (left panel) and hard (right panel) annihilation spectra.

References

Arnaud, M. 2005, preprint astro-ph/0508159

Baltz, E. 2004, preprint astro-ph/0412170

Bartelmann, M. & Schneider, P. 1999, Phys.Rep., 340, 291

Bennett, C.L. et al. 2003, ApJS, 148, 1

Bottino, A. et al. Phys. Rev.D, 68, 043506 [hep-ph/0304080]

Buote, D.A. 2003, preprint astro-ph/0310579

Colafrancesco, S. 2004a, in Frontiers of Cosmology, A. Blanchard & M. Signore Eds., p.75 and p.85

Colafrancesco, S. 2004b, A&A, 422, L23

Colafrancesco, S. 2005, J.Nucl.Phys., in press

Colafrancesco, S. & Mele, B. 2001, ApJ, 562, 24

Colafrancesco, S., Marchegiani, P. & Palladino, E. 2003, A&A, 397, 27

Colafrancesco, S., Profumo, S. & Ullio, P. 2006, preprint[astrop-ph/0607073]

Colafrancesco, S., Profumo, S. & Ullio, P. 2005, A&A, in press [astro-ph/0507575]

Colafrancesco, S. 2005, in 'Near-fields cosmology with dwarf elliptical galaxies', IAU 198 Colloquium Proceedings,
    Eds.Jerjen, H.; Binggeli, B. Cambridge: Cambridge University Press, pp.229-234

Dalal, N. & Keeton, C.R. 2003, preprint astro-ph/0312072

DePetris, M. et al. 2003, ApJ, 574, L119

Gnedin, O.Y. & Primack, J.R. 2004, Ph.Rev.L., 93, 1302

Hu, W. & Dodelson, S. 2002, ARAA, 40, 171

Jungman, G., Kamionkowski, M. & Griest, K. 1996, PhR, 267, 195

Lowenstein, M. & Mushotzky, R.F. 2002, preprint astro-ph/0208090

Macció, A.V. et al 2004, Ph.Rev. D, 69, 3516

Munoz, C. 2004, Int.J.Mod.Phys.A, 19, 3093 [hep-ph/0309346]

Navarro, J., Frenk, C. & White, S.D.M. 1997, ApJ, 490, 493; Navarro, J.F. et al. 2004, MNRAS, 349, 1039

Perlmutter, S. et al. [SCPC] 1999, ApJ, 517, 565

Profumo, S. 2005, Phys. Rev. D in press [astro-ph/0508628]

Riess, A.G. et al. [SSTC] 1998, AJ, 116, 1009

Seljak, U. et al. 2004, preprint astro-ph/0407372

Spergel, D. et al. 2003, ApJS, 148, 175

Totani, T. 2004, preprint astro-ph/0401140

Zwicky, F. 1933, Helv.Phys.Acta, 6, 110